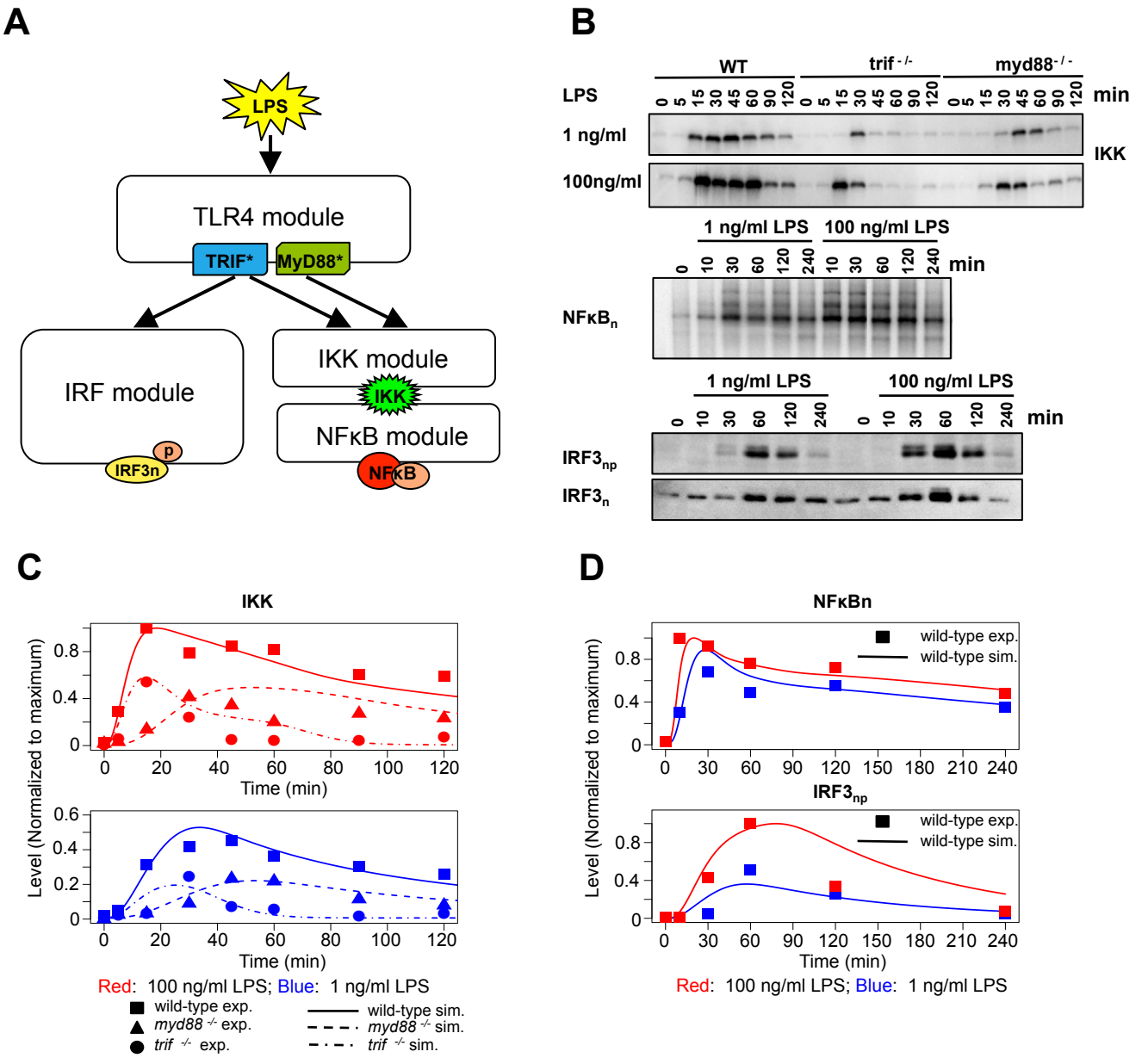

Figure 1. Distinct dynamics in MyD88-dependent and TRIF-dependent pathway, in TLR4 signaling. (*A*) The four modules of the model. (*B*) *Top:* The IKK kinase assay in 1ng/ml and 100ng/ml LPS stimulation for wt, *trif*$^{-/-}$ and *myd88*$^{-/-}$. *Middle:* Nuclear NFκB activity measured by EMSA. *Bottom:* IRF3 activity measured by nuclear phosphorylation. (*C-D*) The model's simulation results against the data quantified from (*B*). "exp." stands for experimental measurements; "sim." stands for simulation result; "mko" stands for *myd88* condition; "tko" stands for *trif*$^{-/-}$condition.

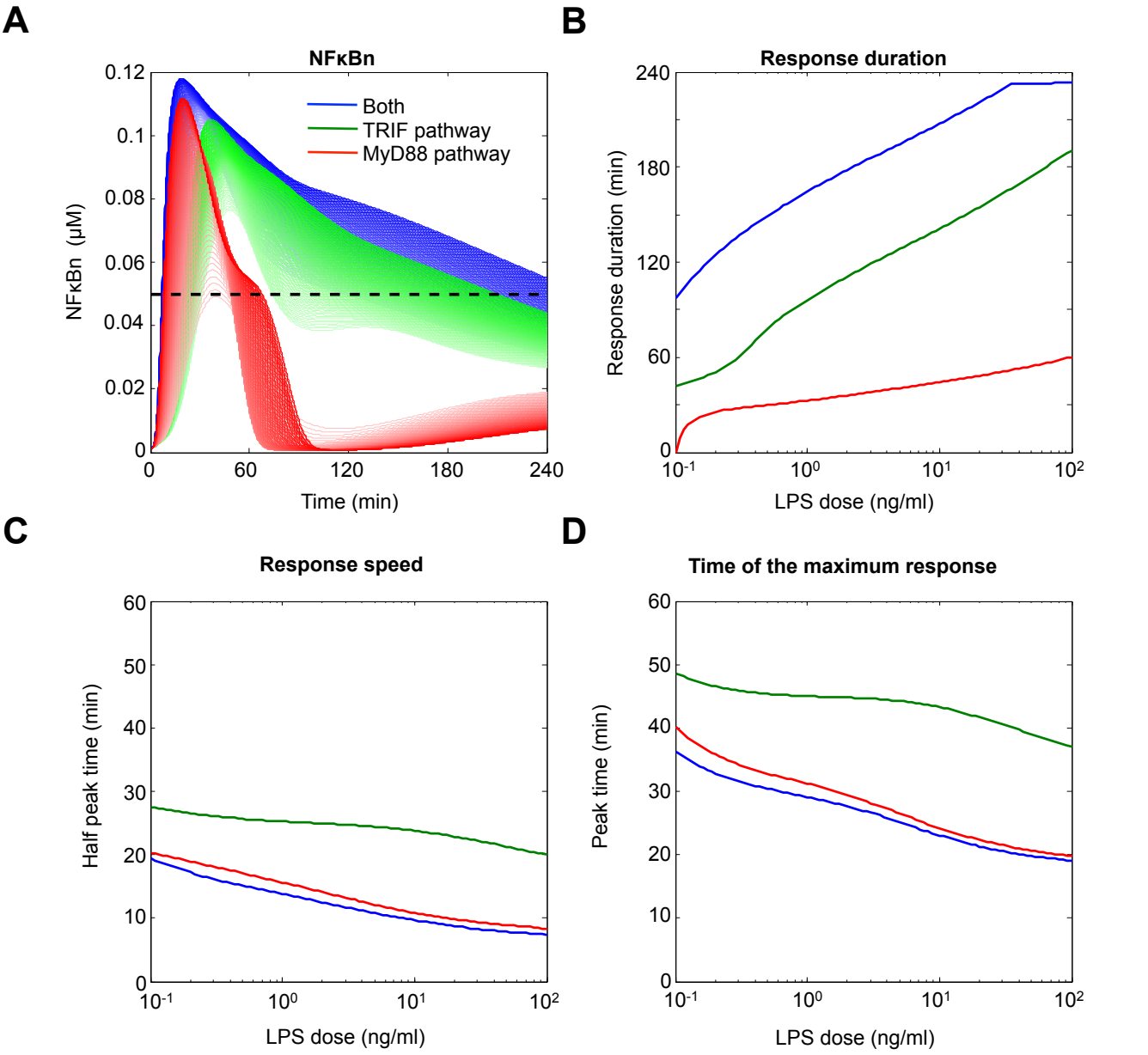

Figure 2. Dynamics features in sub-pathways. (*A*) The NF-κBn time courses in wt (blue), myd88 ko (green) and trif ko (red) conditions, for LPS doses changing from 0.1 ng/ml to 100 ng/ml. (*B*) The NFκBn response duration (i.e. time when NFκBn > 50 nM) vs. the LPS doses. (*C*) The NFκBn response speed (defined by the time NFκBn level first reaches half of the peak level) vs. LPS doses. (*D*). The NF-κBn peak time vs. LPS doses.

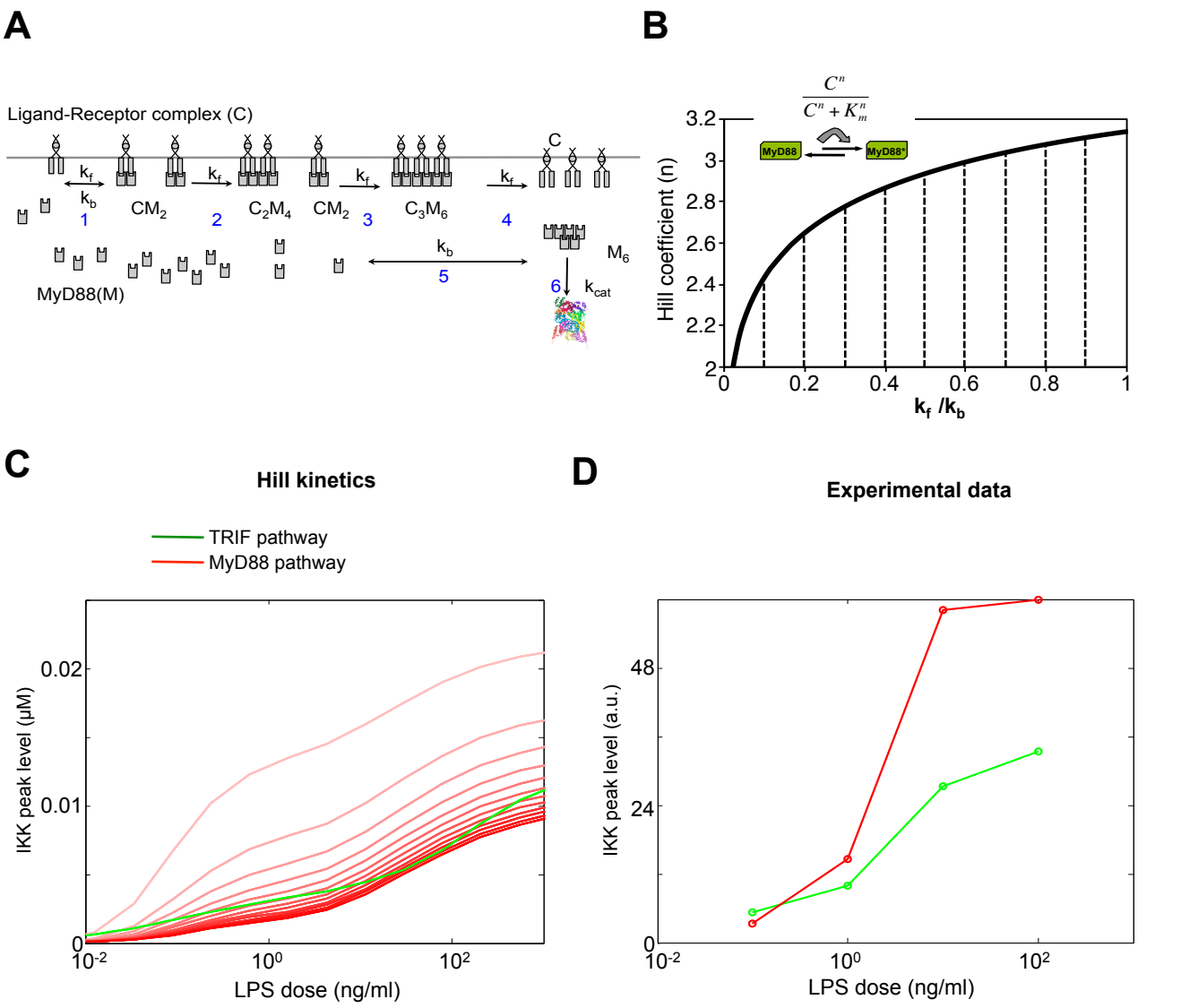

Figure 3. Signalosome affects IKK dynamics. (*A*) The MyDDosome assemble model. (*B*) The hill coefficient vs. k_f/k_b. (*C*) The IKK peak activity in TRIF and MyD88 knockouts vs. LPS concentration, predicted by model based on Hill kinetics with Hill coefficient from the range when k_f/k_b is from 0.1 to 1 in (*B*). (*D*) Quantification of the peak level from the experimental result in Fig. S4.

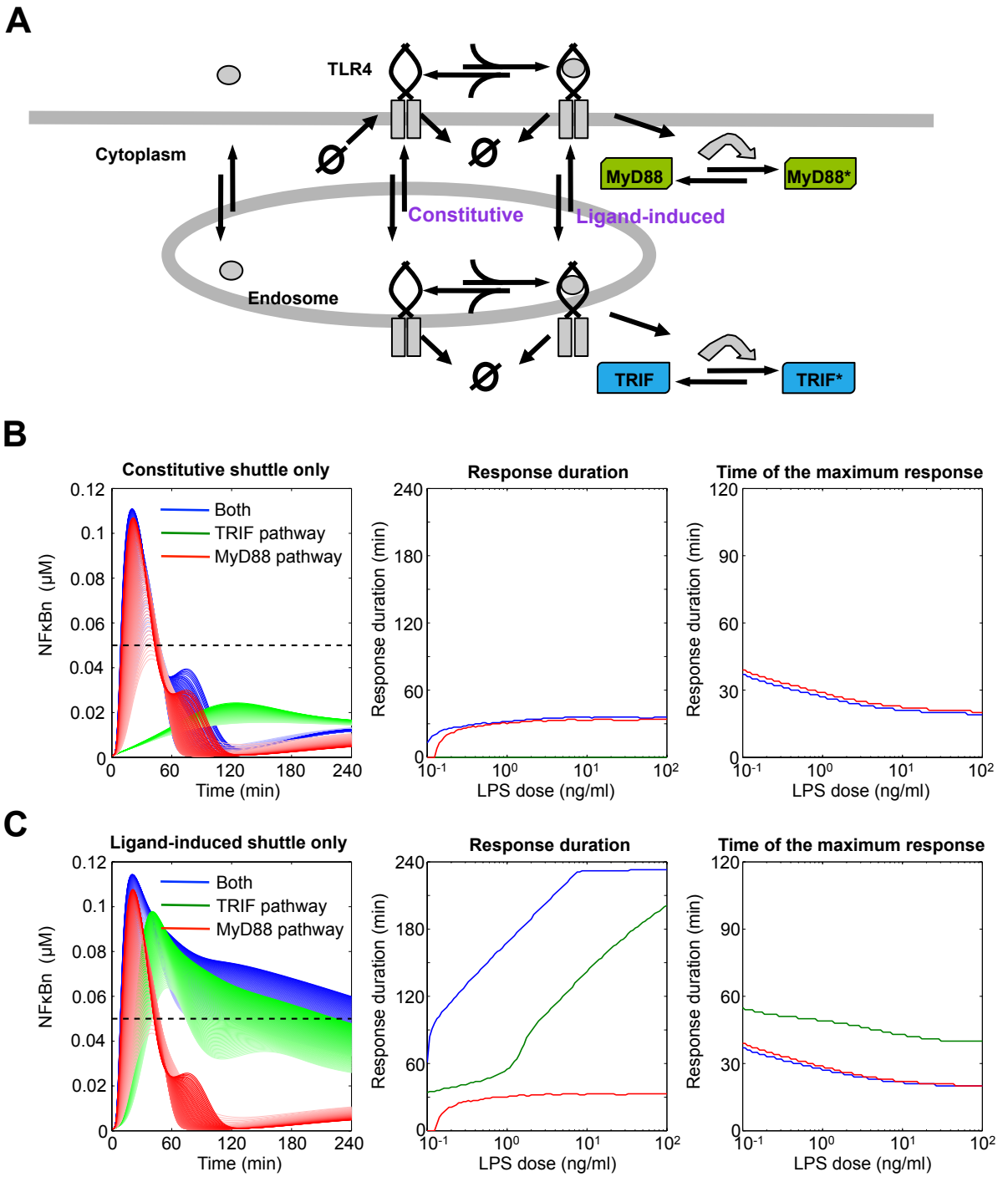

Figure 4. The ligand induced-shuttling is responsible for the duration specificity. (*A*) Two receptor shuttling processes, the constitutive shuttling and the ligand-induced shuttling, are labeled in the part of the model. (*B-C*) The NFκBn time courses (*left*), responses duration (middle) and peak time dose responses in constitutive shuttle only condition (*B*) and ligand-induced shuttle only condition (*C*).

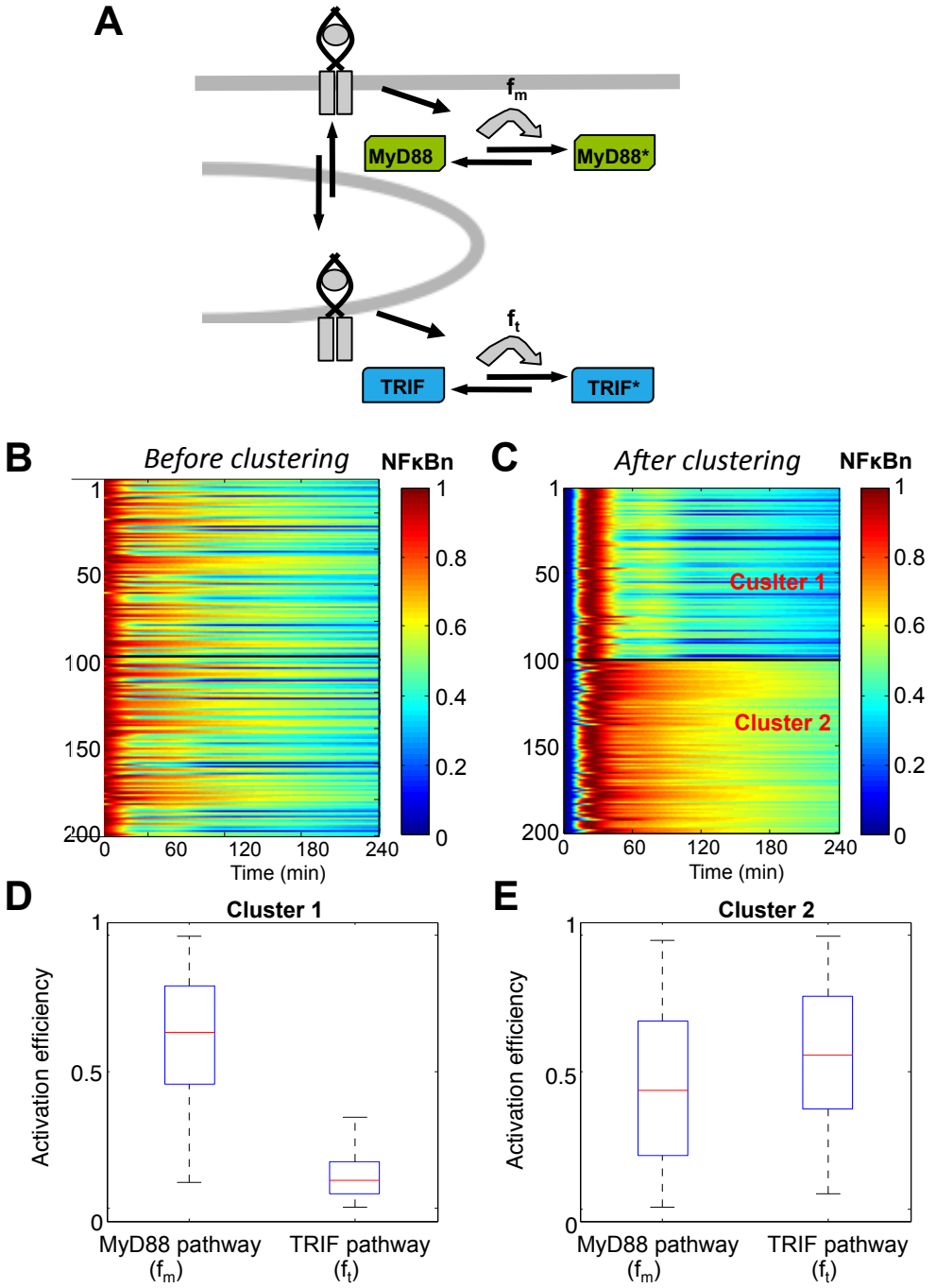

Figure 5. Simulating two clusters of NFκB dynamics in single cell. (*A*) Illustrate the two random fraction parameters in the model. 200 simulations of NF-κBn dynamics before clustering (*B*) and after clustering (*C*). (*D-E*) The boxplot of the fraction parameters in these two clusters.

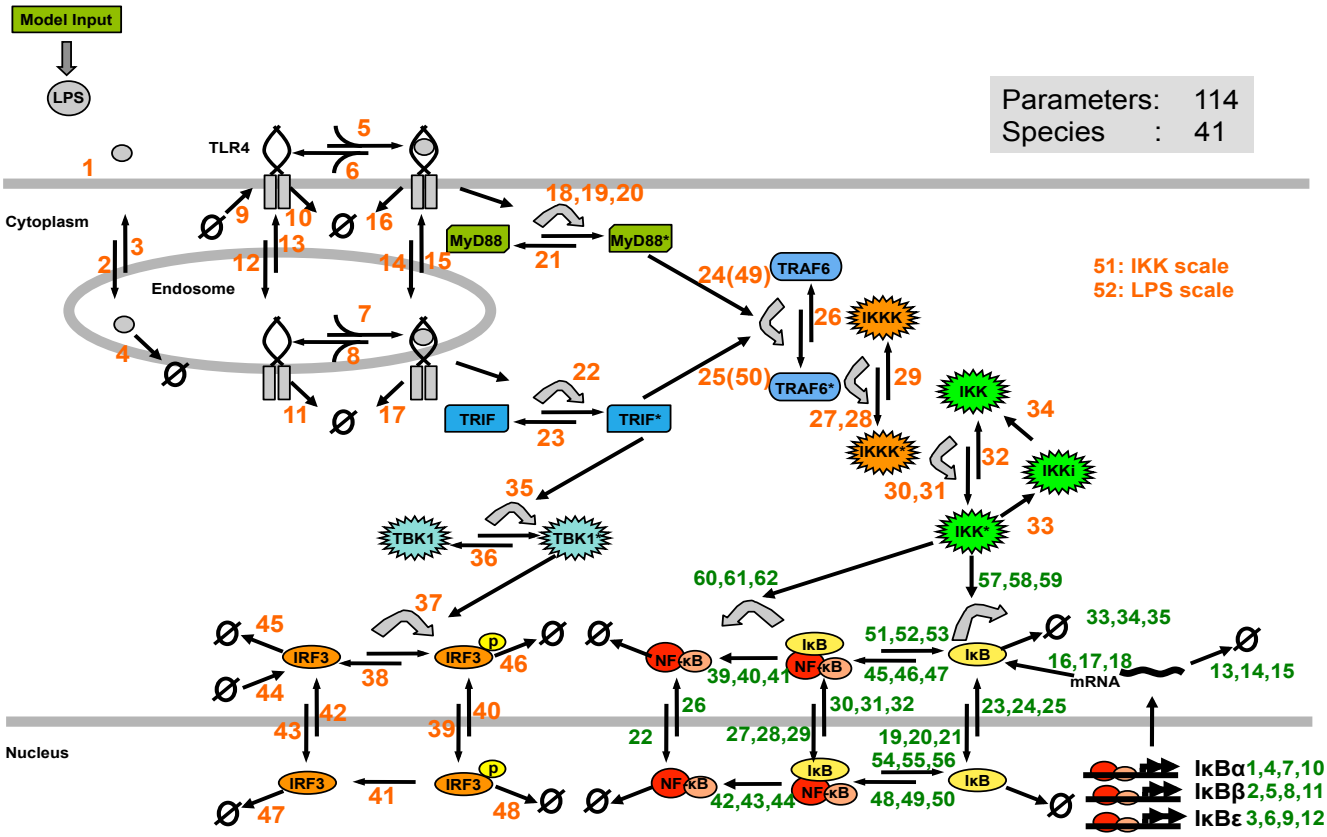

Figure S1. Schematic diagram of the model reaction network. The model is comprised of four modules that are colored by square blocks. The numbers adjacent to the reaction arrows indicate model parameters, which are listed in supplemental table.

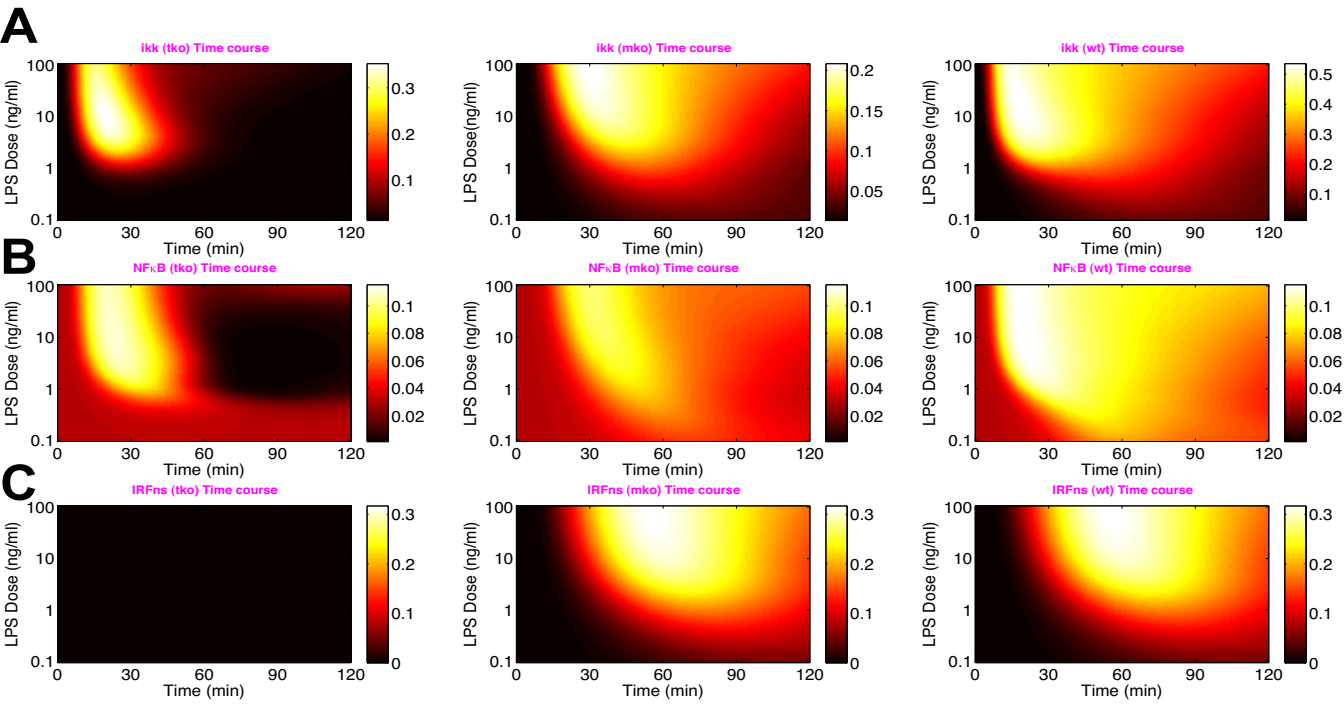

Figure S2. Dose-responses predicted by the model for wt, *trif*$^{-/-}$, and *myd88*$^{-/-}$. Simulated time-course dose response of IKK (*A*), nuclear NFκB (*B*) and IRF3 (*C*) activities in *trif*$^{-/-}$, *myd88*$^{-/-}$ and wt conditions for LPS concentration ranging from 0.1 ng/ml to 100 ng/ml.

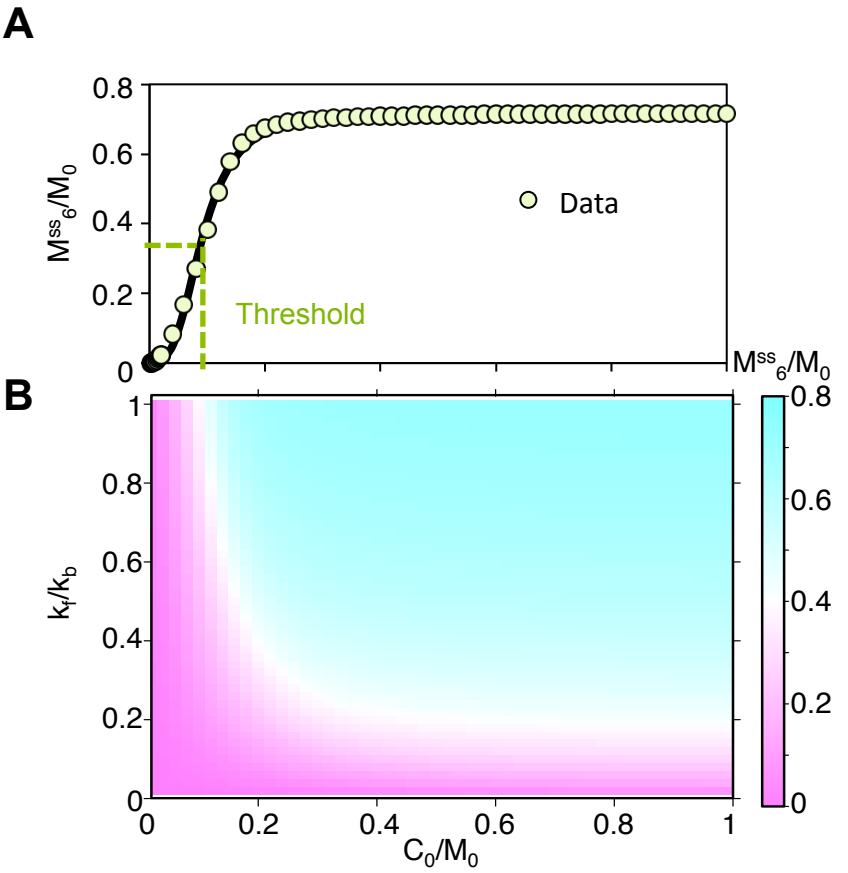

Figure S3. The Myddosome formation model. (*A*) The relative concentrations of M_6^{ss}/M_0 versus the relative input concentration C_0/M_0 in the upper left panel (dots). Parameters are k_f=1, k_b=0.1 and M_0=1. The relationship can be fitted by a Hill equation with Hill constant n = 3.0 (solid line). (*B*) The dose-response of M^{ss}_6/M_0 to C_0/M_0, by varying the fraction k_f/k_b by changing k_f only.

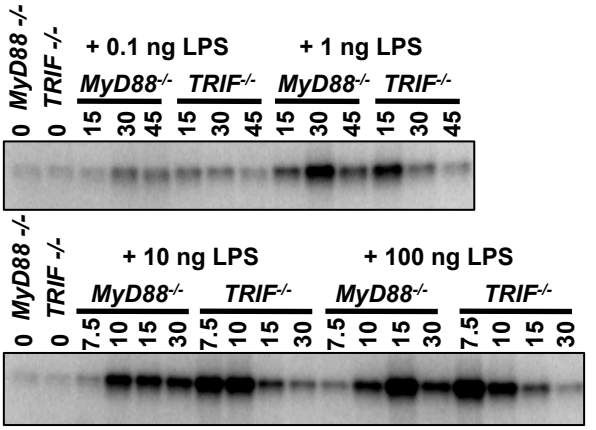

Figure S4. The measurements of IKK activity (*left*) and quantification of the peak level (*right*).

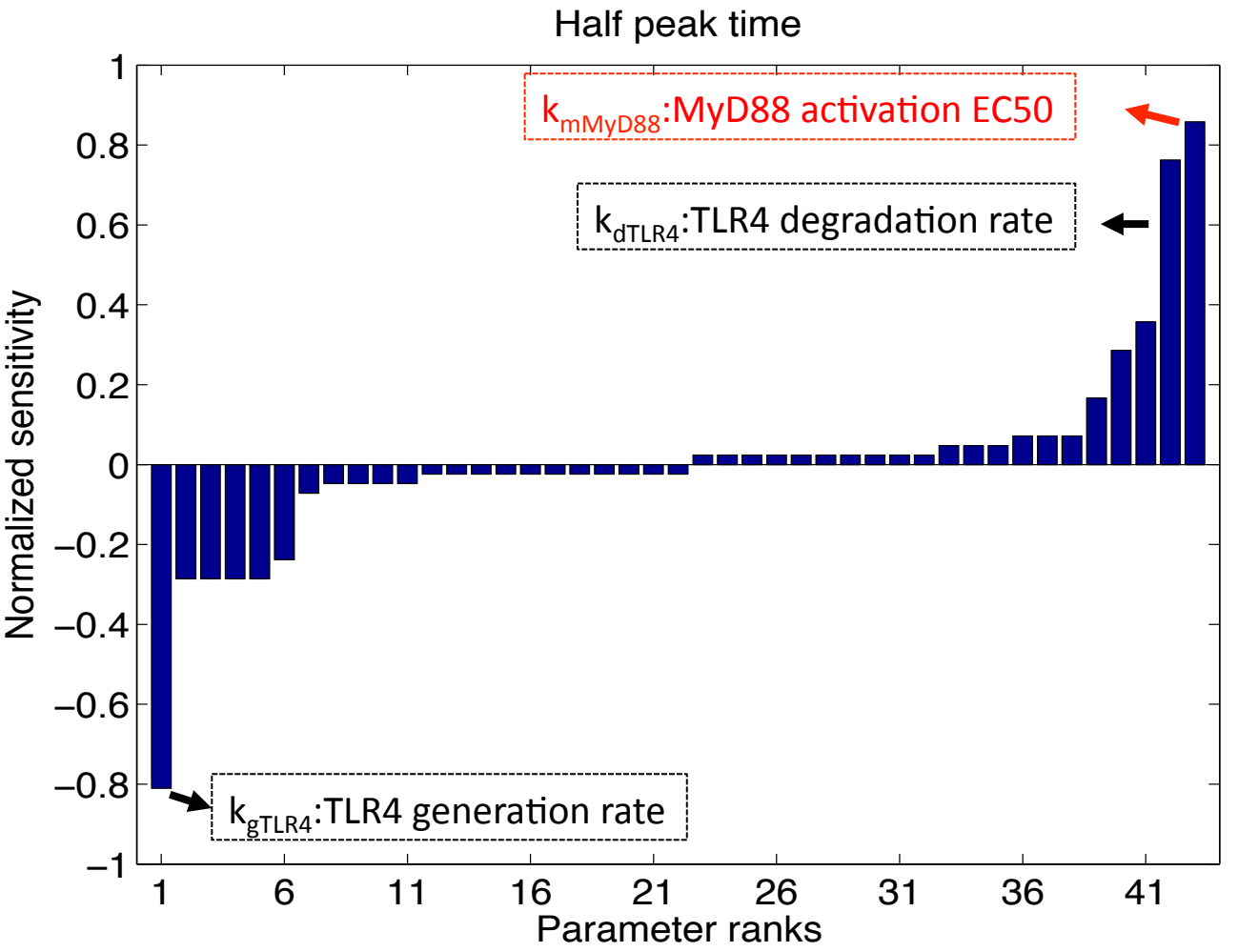

Figure S5. Sensitivity analysis of the NFκB response time. Only those parameters have non-zero sensitivity are plotted in this figure.

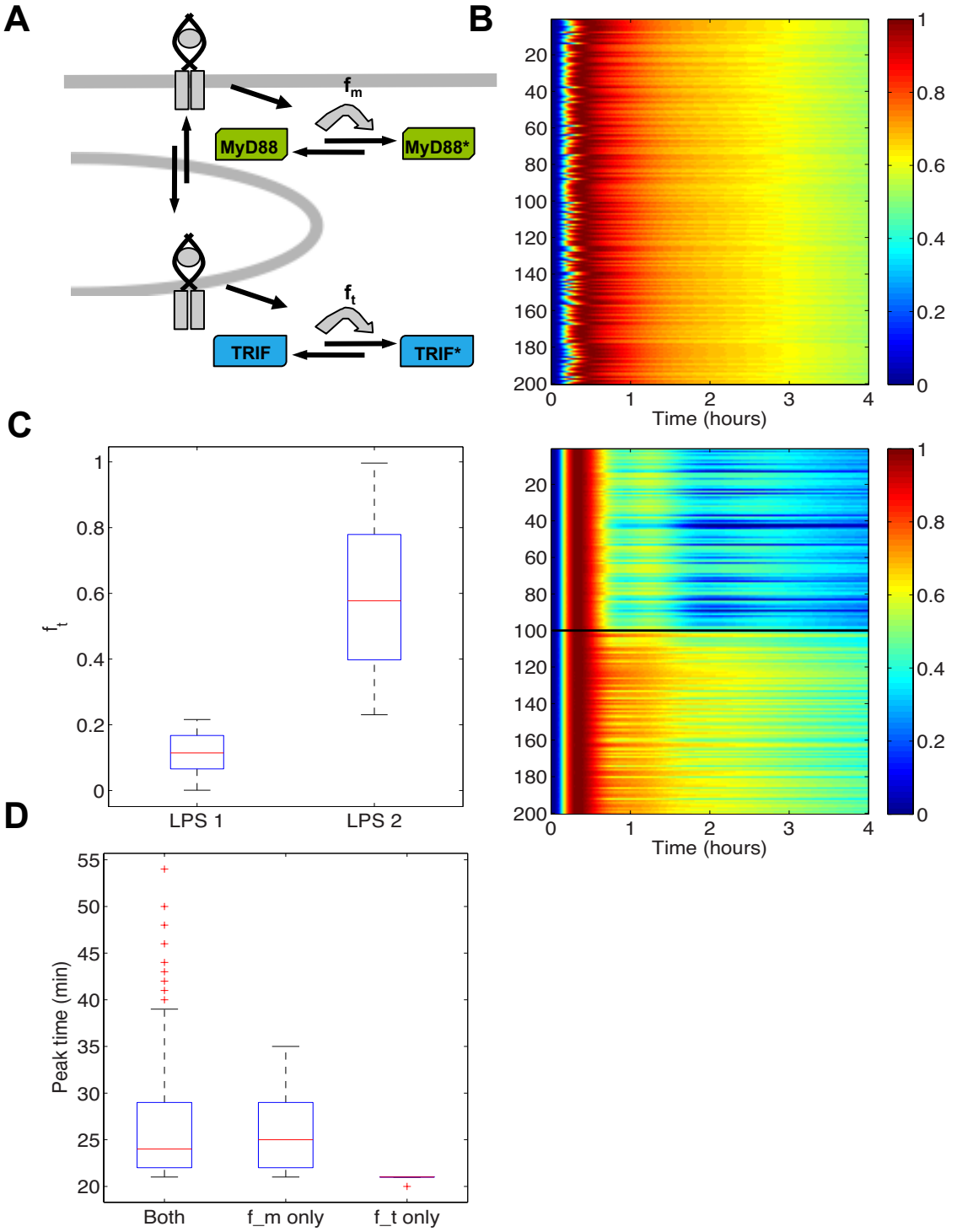

Figure S6. Stochasticity in activation of TRIF-dependent pathway is responsible for the two clusters of LPS responses; Variability in MyD88-dependent pathway contributes to the heterogeneity in the peak response time. Heat-map of the 200 simulations when randomized the fraction of activation in MyD88 activation (*B*) or TRIF activation (*C, right*). Boxplot of f_m in LPS1 and LPS2 is shown in (*C left)*. (*D*) Compare the peak time distributions among the three conditions: 1) randomize both f_m and f_t, 2) randomize f_m only and 3) randomize f_t only.